BULLETIN OF THE POLISH ACADEMY OF SCIENCES
TECHNICAL SCIENCES, Vol. 64, No. 2, 2016
DOI: 10.1515/bpasts-2016-0050

Hypothetical analysis for peristaltic transport of metallic nanoparticles in an inclined annulus with variable viscosity

S. NADEEM and H. SADAF*

Department of Mathematics, Quaid-i-Azam University 45320, Islamabad 44000 Pakistan

Abstract. The main objective of this article is to present a mathematical model for peristaltic transport in an inclined annulus. In this analysis, two-dimensional flow of a viscous nanofluid is observed in an inclined annulus with variable viscosity. Copper as nanoparticle with blood as its base fluid has been considered. The inner tube is unifom or rigid, while the outer tube takes a sinusoidal wave. Governing equations are solved under the well-known assumptions of low Reynolds number and long-wavelength. Exact solutions have been established for both velocity and nanoparticle temperature. The features of the peristaltic motion are explored by plotting graphs and discussed in detail.

Key words: inclined annulus, viscous nanofluid, peristaltic flow, variable viscosity, exact solution.

1. Introduction

Fluid cooling and heating are important in many biomedical and in industrial fields, such as transportation, power and manufacturing. Effective cooling procedures are required for cooling any type of high energy devices. Low thermal conductivity of the conventional heat transfer fluids, such as water, is measured a primary limitation in increasing the performance of such thermal systems. An advanced technique for enhancement of heat transfer by nanoscale particle spread in a base fluid, known as a nanofluid (Choi, [1]). Kuznetsov and Nield [2] described the natural convective boundary layer flow of nanofluid past a rigid flat plate. Sadik and Pramuanjaroenkij [3] reported the review of convective heat transfer enhancement with nanofluids. Nadeem et al. [4] gives the theoretical analysis of Cu-blood nanofluid in a curved channel. Ellahi et al. [5] discussed series solutions of non-Newtonian nanofluids with Reynolds'model and Vogel's model by using the homotopy analysis method. A large number of papers are presented which deal with the study of nanofluid and its uses [6–11].

Peristaltic flow is now an important research area due to its huge applications in physiology and engineering. Peristalsis is basically a mechanism which is produced by successive waves of contractions pushing their fluid forward. Such flows find several uses in physiology, e.g. swallowing of food through the esophagus, sanitary fluids, corrosive fluids, locomotion of some warms and fluids in lymphatic vessels [12–13].

The endoscope or catheter is a very useful instrument, determining the real reasons responsible for many problems in the human organs, in which the fluid is transported by peristaltic pumping such as small intestine, stomach etc. Nadeem et al. [14] discussed the analysis of peristaltic flow for a Prandtl fluid model in an endoscope. Mekheimer and Elmaboud [15] explained the effect of heat transfer and magnetic field on peristaltic transport of a Newtonian fluid in a vertical annulus. Nadeem and Akbar [16] discussed temperature dependent viscosity on peristaltic transport of a Newtonian fluid in an endoscope. Elmaboud [17] described the features of induced magnetic field on peristaltic flow in an annulus.

Nevertheless, no effort has been made yet to discuss the peristaltic motion through an inclined annulus with nano particles. The main goal of this analysis is to study the fluid motion in an inclined annulus with peristaltic walls. The problem is first modeled and then exact solution is calculated for the resultant equation. The results for velocity profile, pressure gradient, pressure rise and stream function have been depicted for several values of the parameters. Numerical results for velocity profile are also presented (see Table 1).

2. Mathematical model

We have considered the peristaltic motion for the two dimensional flow of an incompressible viscous nanofluid in an inclined annulus. The equations for conservation of mass and momentum can be written as

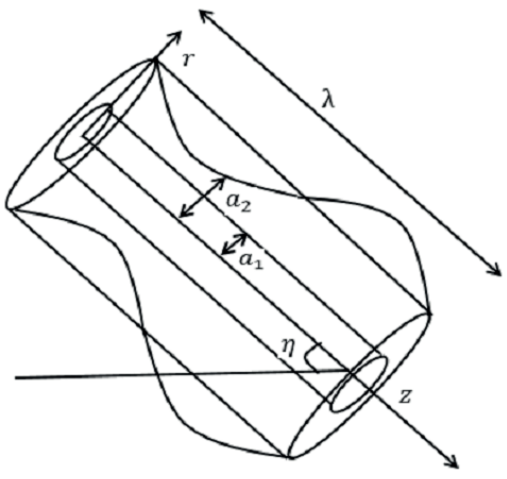

Geometry of the problem

*e-mail: hsadafqau@gmail.com

$$\frac{\partial \tilde{U}}{\partial \tilde{R}} + \frac{\tilde{U}}{\tilde{R}} + \frac{\partial \tilde{W}}{\partial \tilde{Z}} = 0, \tag{1}$$

$$\begin{aligned}
\rho_{nf}\left(\frac{\partial \tilde{U}}{\partial \tilde{t}} + \tilde{U}\frac{\partial \tilde{U}}{\partial \tilde{R}} + \tilde{W}\frac{\partial \tilde{U}}{\partial \tilde{Z}}\right) &= \\
= -\frac{\partial \tilde{P}}{\partial \tilde{R}} + \frac{1}{\tilde{R}}\frac{\partial}{\partial \tilde{R}}\left(2\mu_{nf}\tilde{R}\frac{\partial \tilde{U}}{\partial \tilde{R}}\right) & \\
-\frac{1}{\tilde{R}}\left(\frac{2\mu_{nf}\tilde{U}}{\tilde{R}}\right) + \frac{\partial}{\partial \tilde{Z}}\left(\mu_{nf}\left(\frac{\partial \tilde{W}}{\partial \tilde{R}} + \frac{\partial \tilde{U}}{\partial \tilde{Z}}\right)\right) & \\
-(\rho\beta)_{nf} g(\tilde{T} - T_1)\cos\eta, &
\end{aligned} \tag{2}$$

$$\begin{aligned}
\rho_{nf}\left(\frac{\partial \tilde{W}}{\partial \tilde{t}} + \tilde{U}\frac{\partial \tilde{W}}{\partial \tilde{R}} + \tilde{W}\frac{\partial \tilde{W}}{\partial \tilde{Z}}\right) &= \\
= -\frac{\partial \tilde{P}}{\partial \tilde{Z}} + \frac{1}{\tilde{R}}\frac{\partial}{\partial \tilde{R}}\left(\tilde{R}\mu_{nf}\left(\frac{\partial \tilde{W}}{\partial \tilde{R}} + \frac{\partial \tilde{U}}{\partial \tilde{Z}}\right)\right) & \\
+\frac{\partial}{\partial \tilde{Z}}\left(2\mu_{nf}\frac{\partial \tilde{W}}{\partial \tilde{Z}}\right) + (\rho\beta)_{nf} g(\tilde{T} - T_1)\sin\eta, &
\end{aligned} \tag{3}$$

$$\begin{aligned}
(\rho c_p)_{nf}\left(\frac{\partial \tilde{T}}{\partial \tilde{t}} + \tilde{U}\frac{\partial \tilde{T}}{\partial \tilde{R}} + \tilde{W}\frac{\partial \tilde{T}}{\partial \tilde{Z}}\right) = & \\
= k_{nf}\left(\frac{\partial^2 \tilde{T}}{\partial \tilde{R}^2} + \frac{1}{\tilde{R}}\frac{\partial \tilde{T}}{\partial \tilde{R}} + \frac{\partial^2 \tilde{T}}{\partial \tilde{Z}^2}\right) + Q_0, &
\end{aligned} \tag{4}$$

where $\tilde{U}, \tilde{W}, \rho_{nf}, \tilde{P}, \mu_{nf}, Q_0, (\rho c_p)_{nf}, \kappa_{nf}$ denote the velocity components in the radial and axial direction, nanofluid density, pressure, viscosity of the nanofluid, Q_0 denote constant of heat absorption parameter, the heat capacity of nanofluid and thermal conductivity of the nanofluid defined as follow [15]

$$\begin{aligned}
\rho_{nf} &= (1-\phi)\rho_f + \phi\rho_s, \\
(\rho c_p)_{nf} &= (1-\phi)(\rho c_p)_f + \phi(\rho c_p)_s, \\
\alpha_{nf} &= \frac{\kappa_{nf}}{(\rho c_p)_{nf}},\ (\rho\beta)_{nf} = (1-\phi)\rho_f\beta_f + \phi\rho_s\beta_s, \\
\mu_{nf} &= \frac{\mu_f(T)}{(1-\phi)^{2.5}},\ \mu_f(T) = \mu_0 e^{-\alpha(T-T_1)}, \\
\frac{\kappa_{nf}}{\kappa_f} &= \frac{(\kappa_s + 2\kappa_f) - 2\phi(\kappa_f - \kappa_s)}{(\kappa_s + 2\kappa_f) + \phi(\kappa_f - \kappa_s)}.
\end{aligned} \tag{5}$$

The transformations between the two frames are

$$\tilde{r} = \tilde{R},\ \tilde{z} = \tilde{Z} - c\tilde{t},\ \tilde{u} = \tilde{U},\ \tilde{w} = \tilde{W} - c. \tag{6}$$

The appropriate boundary conditions are defined as

$$\begin{aligned}
\tilde{W} &= 0,\ at\ \tilde{R} = \tilde{R}_1,\ \tilde{W} = 0 \text{ at} \\
\tilde{R} &= \tilde{R}_2 = a_2 + a_2\epsilon\sin\frac{2\pi}{\lambda}(\tilde{Z} - c\tilde{t}), \\
\bar{T} &= \bar{T}_0 \text{ at } \tilde{R} = \tilde{R}_1,\ \bar{T} = \bar{T}_1 \text{ at } \tilde{R} = \tilde{R}_2.
\end{aligned} \tag{7}$$

Introducing the dimensionless variables

$$\begin{aligned}
R &= \frac{\tilde{R}}{a_2},\ r = \frac{\tilde{r}}{a_2},\ Z = \frac{\tilde{Z}}{\lambda},\ z = \frac{\tilde{z}}{\lambda},\ W = \frac{\tilde{W}}{c}, \\
& w = \frac{\tilde{w}}{c},\ U = \frac{\lambda\tilde{U}}{a_2 c},\ u = \frac{\lambda\tilde{u}}{a_2 c}, \\
p &= \frac{a_2^2\tilde{p}}{c\lambda\mu_0},\ \delta = \frac{a_2}{\lambda},\ t = \frac{c\tilde{t}}{\lambda},\ R_e = \frac{ac\rho_f}{\mu_0}, \\
& r_1 = \frac{\tilde{r}_1}{a_2} = \frac{a_1}{a_2} = \xi,\ \theta = \frac{\tilde{T} - \tilde{T}_1}{\tilde{T}_0 - \tilde{T}_1}, \\
\mathrm{B} &= \frac{Q_0 a^2}{\kappa_f(\tilde{T}_0 - \tilde{T}_1)},\ G_r = \frac{g\beta_f\rho_f a^2(\tilde{T}_0 - \tilde{T}_1)}{c\mu_0}, \\
& r_2 = \frac{\tilde{r}_2}{a_2} = 1 + \epsilon\sin(2\pi z), \\
\mu(\theta) &= \frac{\mu_{nf}}{\mu_0},\ s = \tilde{\alpha}(\tilde{T}_0 - \tilde{T}_1).
\end{aligned} \tag{8}$$

Making use of Eqs. (6) and (7) into the Eqs. (1–4), applying the conditions of the low Reynolds number and long wave length approximation, dropping the terms containing Re, δ and higher we get the following equations

$$\frac{\partial p}{\partial r} = 0, \tag{9}$$

$$-\frac{\partial p}{\partial z} + \left[\frac{1}{r}\frac{\partial}{\partial r}\left(r\mu(\theta)\frac{\partial w}{\partial r}\right)\right] + \frac{(\rho\beta)_{nf}}{(\rho\beta)_f}G_r\theta\sin\eta = 0, \tag{10}$$

$$\frac{\alpha_{nf}}{\alpha_f}\left[\frac{1}{r}\frac{\partial \theta}{\partial r} + \frac{\partial^2\theta}{\partial r^2}\right] + B\frac{(\rho c_p)_f}{(\rho c_p)_{nf}} = 0. \tag{11}$$

Eq. (9) shows that p is not the function of r and the boundary conditions to be satisfied can be written as

$$w = -1,\ r = r_2, \text{ and } r = r_1 \tag{12}$$

$$\theta = 1\ at\ r = r_1 = \xi,\ \theta = 0\ at\ r = r_2. \tag{13}$$

3. Reynold's Viscosity Model

The Reynold's model viscosity is defined as [5]

$$\mu(\theta) = e^{-s\theta} \tag{14}$$

where s is the Reynold's model coefficient.

4. Solution of the problem

The exact solution of the boundary value problem (9) to (13) is directly written as

$$\theta = -b_3\frac{r^2}{4} + b_4 Log[r] + b_5, \tag{15}$$

$$\begin{aligned} w \;=\; & C_2 - \frac{1}{64}a_2\Big(\frac{1}{6}a_1 G_r r^6 s b_3^2 \sin\eta + \\ & \frac{1}{4}r^2 b_3(-a_1 G_r r^2 s(-7+12Log[r])(\sin\eta)b_4 \\ & +4(8C_1 s + 2\frac{dp}{dz}r^2 s - a_1 G_r r^2 \sin\eta - \\ & - 3a_1 G_r r^2 s(\sin\eta)b_5)) - 4(-a_1 G_r r^2 s \\ & -6Log[r] + 4Log[r]^2)(\sin\eta)b_4^2 + \\ & + 4(1+sb_5)(\frac{dp}{dz}r^2 + 4C_1 Log[r] - \\ & - a_1 G_r r^2(\sin\eta)b_5) + b_4(2s(-\frac{dp}{dz}r^2 + \\ & + 2\frac{dp}{dz}r^2 Log[r] + 4C_1 Log[r]^2) - \\ & - 4a_1 G_r r^2(-1+Log[r])\sin\eta \\ & -2a_1 G_r r^2 s(-3+4Log[r])(\sin\eta)b_5))). \end{aligned} \tag{16}$$

Constants C_1 and C_2 are evaluated by using boundary conditions defined in Eqs. 12 and 13, while the pressure gradient can be obtained from the following relations

$$F = \int_{r_1}^{r_2}(rw)dr. \tag{17}$$

Flow rate in dimensionless form and velocities in terms of stream function relation can be defined as

$$\begin{aligned} Q &= F + \frac{1}{2}(1 + \frac{\epsilon^2}{2} - \xi^2), \\ u &= -\frac{1}{r}\frac{\partial\Psi}{\partial z}, \\ w &= \frac{1}{r}\frac{\partial\Psi}{\partial r}, \end{aligned} \tag{18}$$

whereas the constants are defined in appendix.

Table (a)
Thermo-physical properties of fluid and nanoparticles.

Physical Properties	Blood	Cu
c_p(J/kgK)	3594	385
ρ(kg/m^3)	1063	8933
κ(W/mK)	0.492	400
$\beta\times10^{-5}$(1/K)	0.18	1.67

Table 1
Variation in velocity profile for fixed values of $B = 0.6$, $s = 0.3$, $\epsilon = 0.07$, $Q = 0.53$, $\eta = \frac{\pi}{4}$

s	B	G_r	ϕ	velocity		velocity for ϕ =0	
				$r = 0.11$	$r = 0.12$	$r = 0.11$	$r = 0.12$
0.3	0.1	5	0.11	-2.81008	-2.46406	-2.50268	-2.22043
0.4				-2.89121	-2.52711	-2.5616	-2.26636
0.5				-2.96846	-2.58716	-2.61691	-2.30948
0.6				-3.04233	-2.64458	-2.66906	-2.35016
	0.2			-2.80734	-2.46203	-2.50032	-2.21867
	0.3			-2.80459	-2.46001	-2.49796	-2.21692
	0.4			-2.80185	-2.45798	-2.49561	-2.21516
		5.5		-2.84294	-2.49026	-2.50534	-2.22265
		6		-2.87855	-2.5185	-2.51036	-2.22663
		6.5		-2.91416	-2.54673	-2.51538	-2.23062
			0.12	-2.47659	-2.82571	-2.50032	-2.21867
			0.13	-2.84268	-2.49003	-2.50032	-2.21867
			0.14	-2.85826	-2.50238	-2.50032	-2.21867

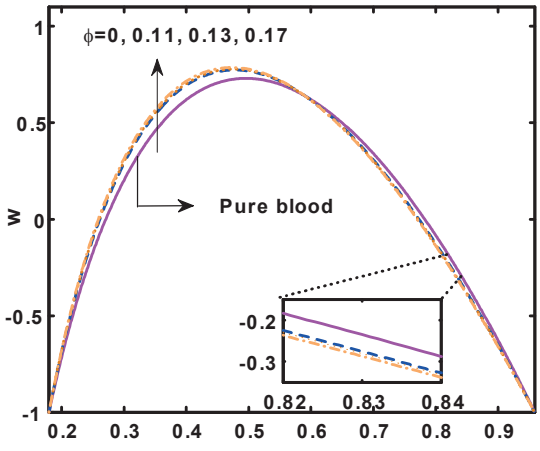

Fig. 1. Velocity profile for fixed parameters are $z = 0.08$, $\xi = 0.18$, $B = 0.6$, $s = 0.3$, $\epsilon = 0.07$, $Q = 0.03$, $\eta = \frac{\pi}{4}$, $G_r = 2$

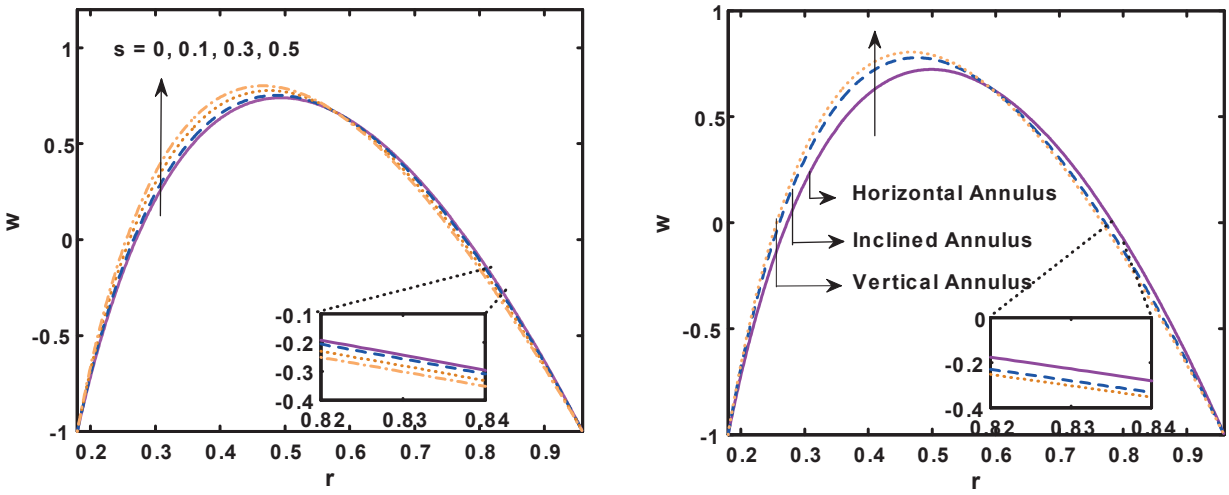

Fig. 2, 3. Velocity profile for 1 for ($\eta = \frac{\pi}{4}$), 2 for ($s = 0.3$) other parameters are $z = 0.08$, $\xi = 0.18$, $B = 0.6$, $\epsilon = 0.07$, $Q = 0.03$, $\phi = 0.13$, $G_r = 2$

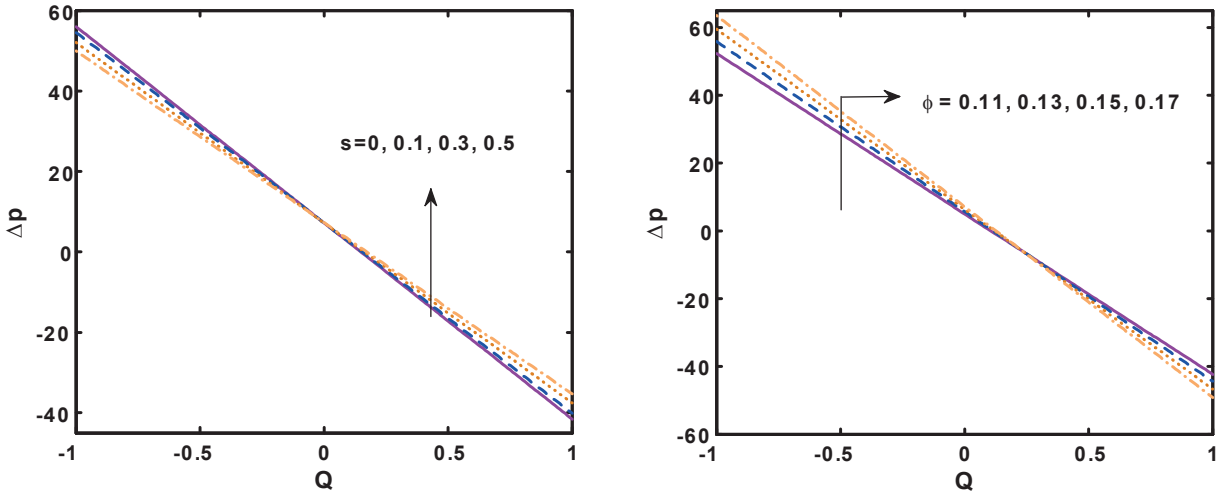

Fig. 4, 5. Pressure rise for 3 for ($\phi = 0.11$), 4 for ($s = 0.1$) other parameters are $\xi = 0.18$, $\eta = \frac{\pi}{4}$, $B = 0.6$, $\epsilon = 0.07$, $G_r = 2$

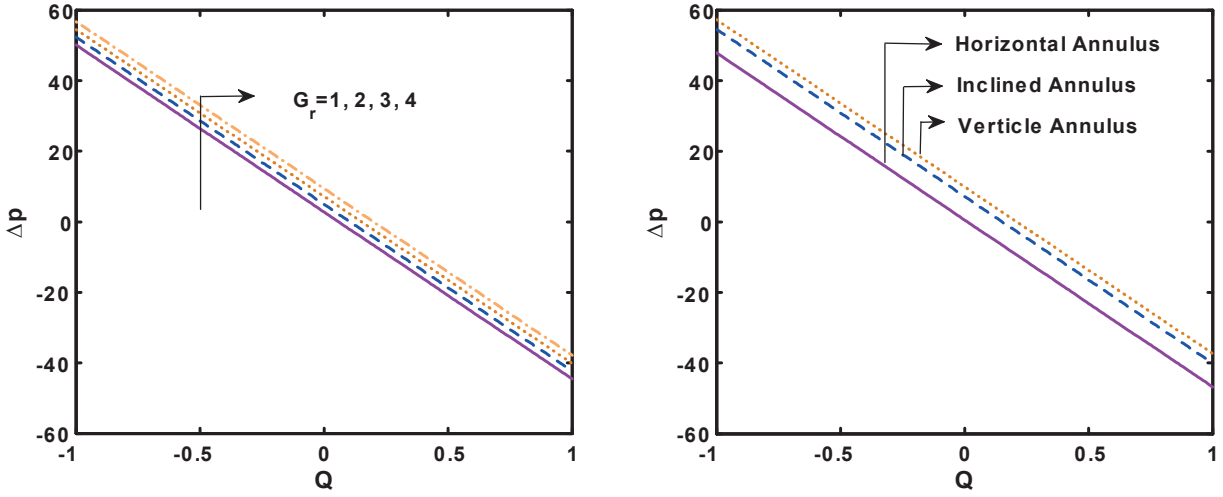

Fig. 6, 7. Pressure rise for 5 for ($\eta = \frac{\pi}{4}$), 6 for ($G_r = 7$) other parameters are $\xi = 0.18$, $B = 0.6$, $\epsilon = 0.07$, $s = 0.5$, $\phi = 0.17$

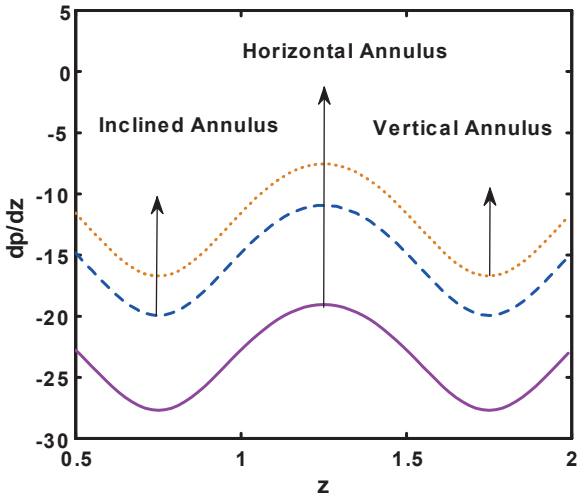

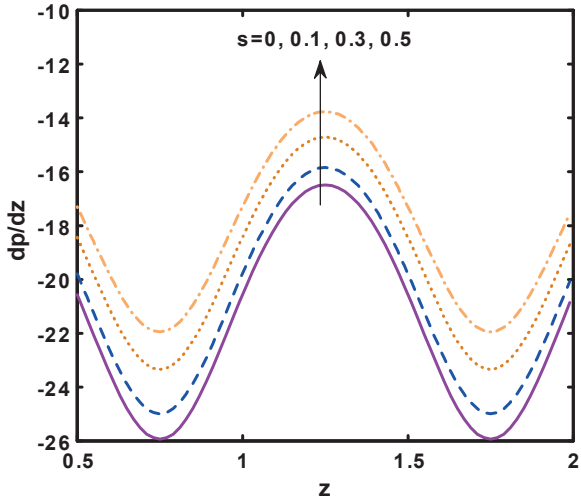

Fig. 8, 9. Pressure gradient 7 for ($s = 0.3$), 8 for ($\eta = \frac{\pi}{4}$) other parameters are $B = 0.6$, $\epsilon = 0.07$, $Q = 0.03$, $\phi = 0.11$, $G_r = 2$

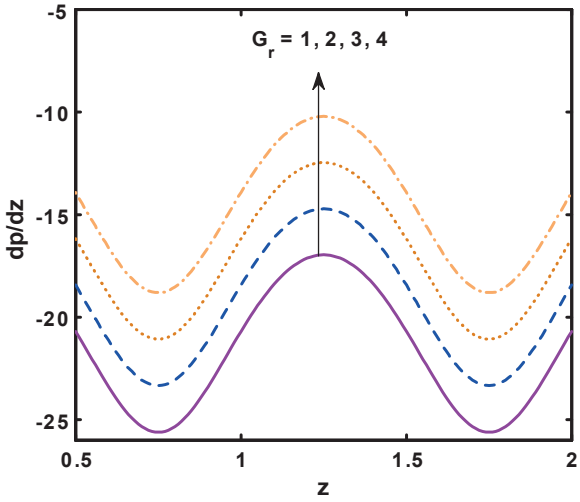

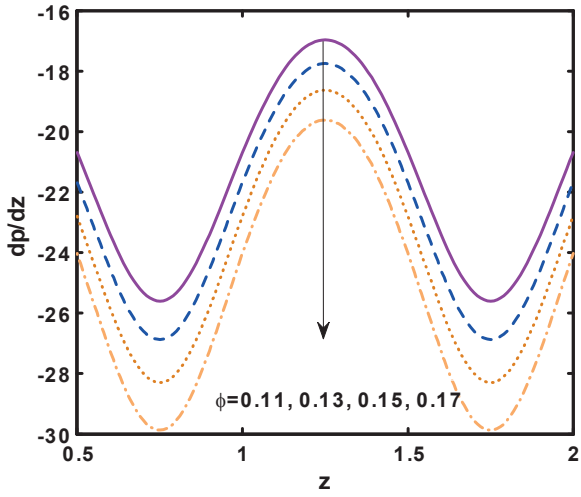

Fig. 10, 11. Pressure gradient 9 for ($\phi = 0.11$), 10 for ($G_r = 2$) other parameters are $B = 0.6$, $\epsilon = 0.07$, $Q = 0.03$, $s = 0.3$, $\xi = 0.18$, $\eta = \frac{\pi}{4}$

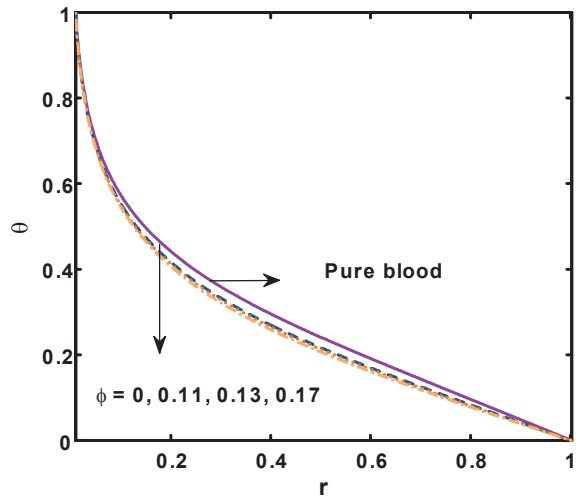

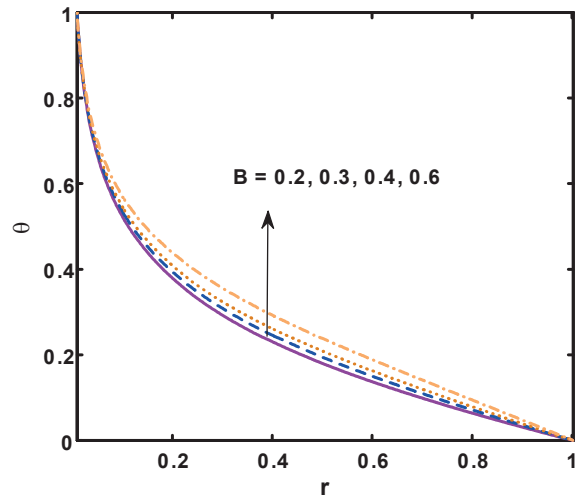

Fig. 12, 13. Temperature profile 9 for ($B = 0.6$), 10 for ($\phi = 0.01$) other parameters are $\xi = 0.01$, $z = 0.06$, $\epsilon = 0.02$

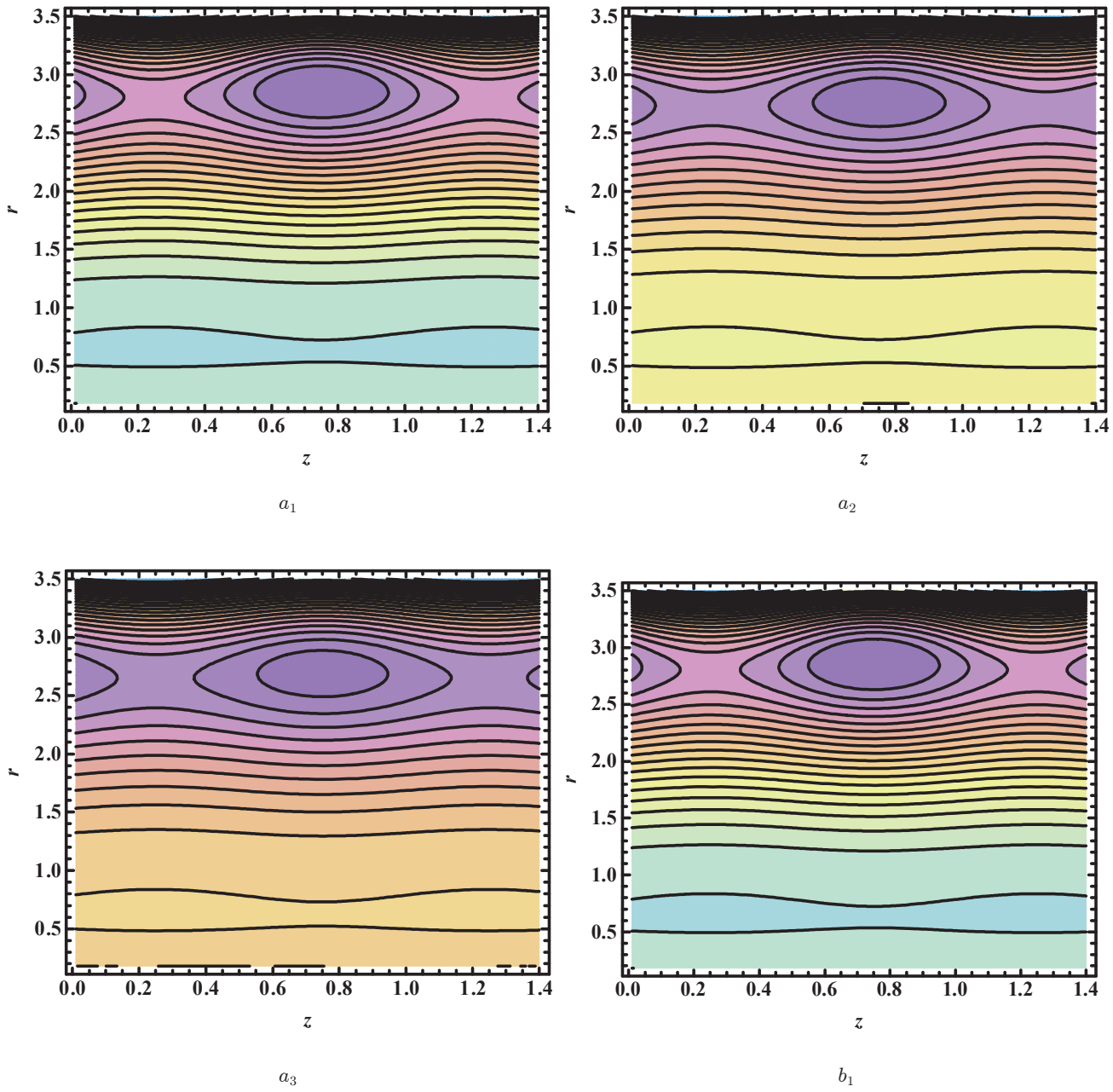

Fig. 14. Streams lines for (a_1) $\phi = 0.09$, (a_2) $\phi = 0.10$, (a_3) $\phi = 0.11$ and the other parameters are $B = 0.6$, $\epsilon = 0.03$, $\xi = 0.18$, $Q = 0.36$, $G_r = 4.1$, $\eta = \frac{\pi}{4}$

Graphical results. This section is devoted to the discussion of graphical results for nanoparticle temperature, fluid velocity, and for stream function. Fig. 1 is the graph of fluid velocity against r, for different values of ϕ. We note that velocity profile increases near the endoscopic tube when we increase nanoparticles concentration into base fluid, however, opposite behavior is depicted near the peristaltic wall. One may observe from Fig. 2 that the velocity for the constant viscosity fluid is lesser as compared to the variable viscosity fluid close to the inner wall, but, we can see quite opposite behavior near the outer wall. Figure 3 are designed to see the behavior of the velocity profile for three different cases, namely, horizontal annulus ($\eta = 0$), inclined annulus (for $\eta = \frac{\pi}{4}$), and vertical annulus (for $\eta = \frac{\pi}{2}$). It is determined that velocity profile near the endoscopic tube increases, when we move from horizontal to the vertical annulus. Figures 4–7 are graphs for pressure rise against Q for different values of s, ϕ, G_r and for different annulus cases. It is perceived from Fig. 4 that pressure rise in the retrograde pumping region ($-1 \leq Q \leq -0.1$) increases when we increase the value of s, whereas reflux occur in the peristaltic as well as in augumented pumping region. It is also depicted from Fig. 4 that pressure rise for the constant viscosity fluid is lesser

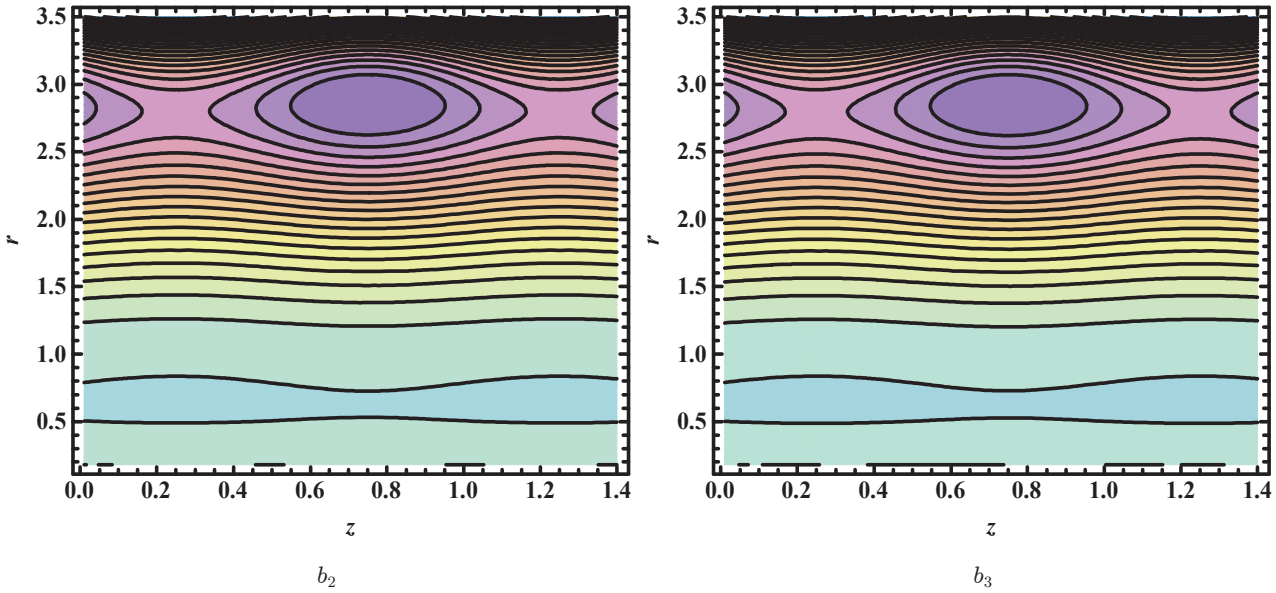

Fig. 15. Streams lines for (b_1) $s = 0.11$, (b_2) $s = 0.13$, (b_3) $s = 0.15$ and the other parameters are $B = 0.6$, $\phi = 0.11$, $\xi = 0.18$, $Q = 0.36$, $G_r = 4.1$, $\eta = \frac{\pi}{4}$, $\epsilon = 0.03$

as compared to the variable viscosity fluid in the peristaltic and augumented pumping region. It is determined from Fig. 5 that pressure rise in the retrograde ($Q < 0$ $\triangle p > 0$) and peristaltic pumping region ($Q > 0$ $\triangle p < 0$) increases with an increase in ϕ, otherwise opposite behavior is detected in the augumented pumping region. Figure 6 shows the graph for different values of G_r, the increase in G_r contributes in enhancing the pressure rise in peristaltic, augumented as well as in retrograde pumping region. Figure 7 is a graph for different values of η, it is determined that pressure rise for the vertical annulus $\eta = \frac{\pi}{2}$ gets the larger values as compared to the horizontal and inclined annulus. Figures 8–11 are graphs for pressure gradient against z for different values of ϕ, G_r, s and η. It is perceived from these figures that in the wider part of the problem or (the endoscope tube) in the regions ($0.5 \leq z \leq 1$, $1.5 \leq z \leq 2$) for Figures (8–11) pressure gradient is small, that is flow can easily pass without imposition of large pressure gradient, whereas in the narrow part of the problem in the intervals ($1.1 \leq z \leq 1.49$) for Figs. (8–11), a much larger pressure gradient is required to maintain the same flux to pass it. This is in well agreement with the physical situation. Moreover, pressure gradient increases for increasing the values of G_r, s and η but, decreases for increasing the values of ϕ. Figure 12 illustrates the influence of ϕ on nanoparticle temperature profile. Increase in nanoparticle concentration decrease in fluid temperature. Basically, high thermal conductivity of the nano fluid plays a key role in the quick dissipation. This justifies that the use of the copper nanoparticle in different types as a coolant. Effects of heat absorption parameter on nanoparticle temperature are shown in Fig. 13. We observe an increase in temperature with a rise in B. The streamlines for different values of volume fraction of the nanoparticle are shown in Fig. 14. We note that by raising ϕ, the number of the bolus reduces but, after that number of the trapped remains same but size of the trapped bolus increases when the value of ϕ is 0.11. The effect of s on trapping is discussed in Fig. 15. We see that number of the trapped boluses remain same but size of the trapped boluses slightly increases.

5. Conclusions

In the current study, we discuss the effects of viscous nanofluid in an inclined annulus. The main conclusion can be concisely as follows

- Velocity profile enhances near the endoscopic tube by increasing values of ϕ, G_r and η .
- Pressure rise and pressure gradient gets the larger values for the vertical annulus.
- Temperature profile increases when we add nano particle into our base fluid.
- Number of trapped bolus increases with an increase in s.

References

[1] S.U.S. Choi, *Enhancing thermal conductivity of fluids with nanoparticles*, in: D.A. Siginer, H.P. Wang (Eds.), *Developments and Applications of Non-Newtonian Flows*, ASME, New York. 66, 99 (1995).

[2] A. V Kuznetsov, A. D. Nield, Natural convective boundary-layer flow of a nanofluid past a vertical plate, Int. J. Thermal Sci. 49, 243–247 (2010).

[3] K. Sadik and A. Pramuanjaroenkij, Review of convective heat transfer enhancement with nanofluids, *Int. J. Heat Mass Trans*. 52, 3187–3196 (2009).
[4] S. Nadeem, H. Sadaf, Theoretical analysis of Cu-blood nanofluid for metachronal wave of cilia motion in a curved channel. *IEEE Tran. Nanobio*., 14, 447–454 (2015).
[5] R. Ellahi, M. Razab, K. Vafaia, Series solutions of non-Newtonian nanofluids with Reynold's model model and Vogel's model by means of the homotopy analysis method, *Math and Comp Modl*. 55, 1876–1891 (2012).
[6] N. S. Akbar, A. W. Butt, CNT suspended nanofluid analysis in a flexible tube with ciliated walls. *Eur. Phy. J. Plus*. 129, 174 (2014).
[7] S. Akram and S. Nadeem, Signifcance of Nanofluid and Partial Slip on the Peristaltic Transport of a Non-Newtonian Fluid with Different Wave Forms. *IEEE Tran. Nanotech*., 13, 375–385(2014).
[8] M. H. M. Yasin, A. Md. Norihan, N. Roslinda, I. Fudziah and P. Ioan, Mixed Convection Boundary Layer Flow Embedded in a Thermally Stratifled Porous Medium Saturated by a Nanofluid, *Adva. Mech. Eng*. 121943 (2013).
[9] S. Nadeem, H. Sadaf, Trapping study of nanofluids in an annulus with cilia, *Aip Ad- vances*. 5, 127204 (2015).
[10] R. Ellahi, The effects of MHD and temperature dependent viscosity on the flow of non- Newtonian nanofluid in a pipe. Analytical solutions. *Appl. Math. Modl*. 37, 1451–1467 (2013).
[11] S. Nadeem, H. Sadaf and A. M. Sadiq, Analysis of Nanoparticles on Peristaltic Flow of Prandtl Fluid Model in an Endoscopy, *Current Nanosci*. 10, 709–721(2014).
[12] T. W. Latham, *Fluid motion in a peristaltic pump*, M.Sc. Thesis, Massachusetts Institute of Technology, Cambridge, 1966.
[13] A. H. Shapiro, M. Y. Ja*erin, S. L.Weinberg, Peristaltic pumping with long wavelengths at low Reynolds number, *J. Fluid. Mech*. 37, 799- 825(1969).
[14] S. Nadeem, H. Sadaf, N. S. Akbar, Analysis of peristaltic flow for a Prandtl fluid model in an endoscope. *J. Power Tech*. 94, 1–11 (2014).
[15] S. Kh. Mekheimer, Y. A. Elmaboud, The influence of heat transfer and magnetic field on peristaltic transport of a Newtonian fluid in a vertical annulus: Application of an endoscope. *Physics Letters* A 372, 1657–1665 (2008).
[16] S. Nadeem, N. S. Akbar, Influence of temperature dependent viscosity on peristaltic transport of a newtonian fluid: Application of an endoscope, *Appl. Math. Comp*. 216, 3606–3619(2010).

6. Appendix

$$b_1 = \frac{\alpha_f}{\alpha_{nf}},\ b_2 = \frac{(\rho c_p)_f}{(\rho c_p)_{nf}},\ b_3 = Bb_1b_2,\ b_4 = -\frac{-4 - b_3 r_1^2 + b_3 r_2^2}{4(Log[r_1] - Log[r_2])},$$

$$b_5 = \frac{-(-b_3 r_2^2 Log[r_1] + 4Log[r_2] + b_3 r_1^2 Log[r_2])}{(4(Log[r_1] - Log[r_2]))}, a_2 = (1-\phi) + \phi\frac{\rho_s\beta_s}{\rho_f\beta_f},\ a_1 = (1-\phi)^{2.5}.$$